

Effect of morphology of second-phase martensite on tensile properties of Fe–0.1C dual phase steels

YOSHIYUKI TOMITA

Department of Metallurgical Engineering, College of Engineering, University of Osaka Prefecture, 4-804 Mozu-Umemachi, Sakai, Osaka 591, Japan

Fe–0.1C steel has been studied to determine the effect of morphology (shape, size and distribution) of the second-phase martensite on the tensile properties of dual phase steels. Retention at an intercritical temperature of 1023 to 1073 K followed by ice–brine quenching (intercritical quenching treatments), whereby martensite appears to surround the ferrite grain, increased strength, but produced an increased yield ratio and decreased ductility. Incorporation of 1223 K direct ice–brine quenching prior to the intercritical quenching treatment at 1053 K gave rise to the distribution of fine spheroidized martensite in a refined ferrite matrix. The heat treatment significantly improved strength and ductility, but produced a somewhat increased yield ratio. Austenitization at a temperature of 1223 K followed by step quenching to 1023 K prior to ice–brine quenching, whereby martensite was randomly scattered in massive form in the ferrite matrix, gave a better combination of strength and ductility and produced a decreased yield ratio. These results are briefly discussed in terms of stress–strain analysis and fractography.

1. Introduction

Dual phase steels with a ferrite and martensite structure offer the potential for greater fuel economy through weight reduction for the same size and cost of product in addition to superior formability when compared to commercially available high strength, low alloy steel (HSLA steel). The enhancement of mechanical properties of the dual-phase steel has therefore been a subject of interest in the last decade that has attracted the attention of automobile and truck manufacturers. Considerable research effort has been directed toward clarifying the mechanical behaviour of dual phase steels [1–9]. Several important points concerning these mechanical properties have been reported. Among these are the importance of the volume fraction of second-phase martensite on strength and ductility [2–6], analysis of strength and elongation based on mixture rules of the volume fraction of martensite and ferrite [3–5] and the effect of the presence of mobile dislocation in the ferrite matrix on continuous yielding [2, 3]. It is not yet, however, clear exactly how morphology (shape, size and distribution) of the second-phase martensite on tensile properties, e.g., yield ratio and ductility of dual phase steels, in spite of the fact that such an effect is regarded as being of major importance for improvement in the formability of the steels [9].

In the present work, Fe–0.1 C steel has been studied to determine the effect of morphology (shape, size and distribution) of second-phase martensite on the tensile properties of the dual phase steels.

2. Experimental procedure

The steels used in the present investigation were Fe–0.1 C and Fe–0.3 C steels whose chemical compositions are given in Table 1. The steels were received as 80 mm diameter hot-rolled bar stock. Fe–0.1 C steel was used to determine the effect of the morphology on the mechanical properties of the dual phase steels. Fe–0.3 C steel was used to study the effect of plastic deformation. The test steels were machined from the bars and each was fully annealed.

In order to change the morphologies of the second-phase martensite, three kinds of heat treatment were conducted as shown in Fig. 1. All the specimens were austenitized in an argon atmosphere tube furnace with a flat zone temperature accuracy of ± 0.5 K.

Tensile tests were performed using a smooth specimen as shown in Fig. 2. The specimen was machined slightly oversized prior to heat treatment. The final dimension was obtained by careful grinding. The specimens were pulled on an Instron machine at a constant strain rate of $3.35 \times 10^{-4} \text{ sec}^{-1}$ at room temperature (293 K). The microstructure was categorized using both optical metallography and thin foil transmission electron microscopy (TEM). The volume fraction of the second-phase martensite was determined using a point counting method in which the specimen was viewed directly on the optical microscope stage. Thin foils were prepared from 1.5 mm thick heat-treated specimens, first by mechanical grinding to a 0.1 mm thickness, then by chemical thinning in a mixed solution of hydrofluoric acid and hydrogen peroxide.

TABLE I Chemical composition of steels (wt %)

Steel	C	Si	Mn	P	S
Fe-0.1 C	0.10	0.20	0.70	0.011	0.019
Fe-0.3 C	0.30	0.22	0.74	0.011	0.017

Finally, the specimens were electropolished in a mixed solution of phosphoric and chromic acids. Quantitative analysis of retained austenite was made by X-ray diffraction measurements using a step scan operated at $0.025^\circ \text{ sec}^{-1}$ with $\text{CoK}\alpha$ radiation [10, 11]. The combination of peaks chosen for the analysis included $(211)\alpha$, $(220)\gamma$, and $(311)\gamma$ [11]. Fractographic morphologies were characterized using a scanning electron microscope (SEM).

3. Results and discussion

3.1. Microstructure

Fig. 3 shows representative optical micrographs of steels processed by the three kinds of heat treatment. Optical microscopy revealed that martensite appeared to surround the ferrite grain when treated by holding it at an intercritical temperature followed by ice-brine quenching (intercritical quenching treatments; heat treatment A). Optical microscopy also revealed that incorporation of 1223 K direct ice-brine quenching prior to heat treatment A (heat treatment B) gave rise to a distribution of fine spheroidized martensite in a refined ferrite matrix. Further optical microscopy revealed that an austenitizing temperature of 1223 K followed by step quenching to 1023 K prior to ice-brine quenching (heat treatment C) produced a microstructure in which martensite was scattered in massive form in the ferrite matrix. The substructure of the

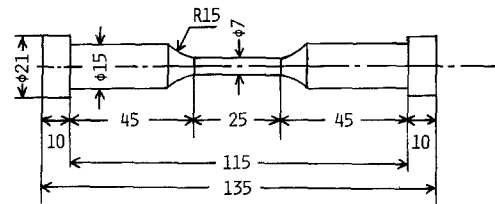


Figure 2 Shape and dimensions (in mm) of tensile specimen.

dual-phase steels was investigated by TEM. TEM observations in the martensite region revealed that the martensitic structure was similar in all cases and that the martensite possessed parallel lath morphology (Fig. 4a). TEM observations in the ferrite region revealed that when heat treated by the heat treatment A method, a fine cell structure was found around martensite (Fig. 4b), while the formation of subgrains which is thought to be formed by the recovery of the cell structure was observed when heat treated by the heat treatment B method (Fig. 4c) and a tangle of dislocations was found in the vicinity of martensite when treated by the heat treatment C method (Fig. 4d). TEM also revealed that no appreciable fine cementite was found independent of heat treatments. While the retained austenite was quantitatively measured by X-ray, no appreciable retained austenite (γ) was detectable independent of heat treatments ($\gamma < 1.5 \text{ vol } \%$).

3.2. Tensile properties

Tensile properties of the dual phase steels processed by various heat treatments are given along with the volume fraction of martensite in Table II. The results obtained from Table II are summarized as follows: (1) heat treatment A increased strength and ductility (elongation and reduction in area) with increased volume fraction of martensite and maintained a high yield ratio independent of the volume fraction of martensite; (2) the heat treatment B method significantly increased strength, ductility, but produced a somewhat increased yield ratio; and (3) heat treatment C gave the best combination of mechanical properties. This heat treatment produced a decreased yield ratio.

3.3. Stress-strain analysis

It can be seen from the present results that yield ratio of the dual phase steel processed by heat treatment A compared to the other two steels is larger at a similar volume fraction level. This probably should be affected by the plastic-deformation behaviour which is changed by morphology of the second-phase martensite. In order to elucidate the plastic-deformation behaviour of the dual phase steels, the stress-strain curves of the dual phase steels were analysed. The modified Crussard-Jaoul (C-J) analysis [12, 13] has been applied to analyse the stress-strain curves of the dual phase steels in this investigation because the method is suitable for the dual phase steel in which increased work-hardening rapidly occurs without exhibiting the discontinuous-yield phenomenon. In the modified C-J analysis, the stress-strain relationship

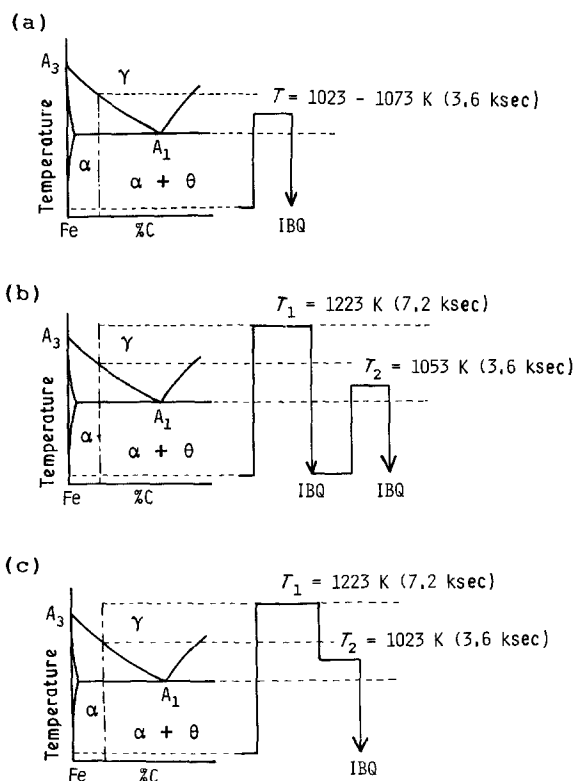


Figure 1 Schematic representation of the three kinds of heat treatment studied (a) A, (b) B, (c) C. (IBQ ice brine quench).

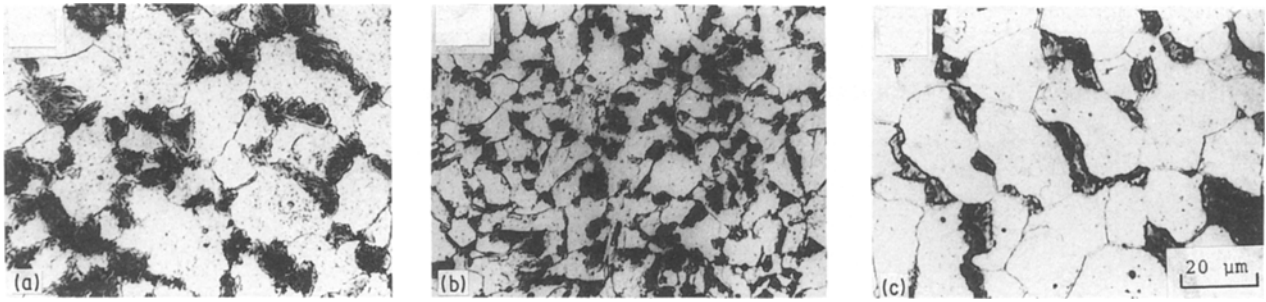


Figure 3 Microstructure of dual phase steels (optical). (a) steel processed by heat treatment A - 2 ($T = 1053\text{ K}$); (b) steel processed by heat treatment B; (c) steel processed by heat treatment C.

becomes

$$\varepsilon = \varepsilon_0 + c\sigma^m \quad (1)$$

where σ is the true stress; ε the true strain; ε_0 the initial true strain, m the work-hardening exponent; and c the material constant. The logarithmic form of Equation 1, differentiated with respect to ε , is

$$\ln(d\sigma/d\varepsilon) = (1 - m) \ln \sigma - \ln(cm) \quad (2)$$

The slope of the $\ln(d\sigma/d\varepsilon)$ against $\ln \sigma$ curve equals $(1 - m)$, while its intersection with $\ln \sigma = 0$ provided $\ln(cm)$.

Figs 5 and 6 show $\ln(d\sigma/d\varepsilon)$ against $\ln \sigma$ curves for dual phase steels processed by various heat treatments. As can be seen from these figures, all the dual

phase steels deformed in two stages [13]. A representative slope of the first stage before the knee (arrowed in Figs 5 and 6) and that of the second stages after the knee are shown in Table III. In Table III the slope of a single phase of ferrite and that of a mixed structure of martensite and ferrite are also shown. In this case, the slope of single phase of ferrite was approximated by that of a fully annealed Fe-0.1 C steel (FA steel) and the slope of a single phase of martensite was approximated by that of a fully martensitic steel containing 0.30 wt % C steel (Fe-0.3 C steel in Table I). The carbon content of the martensite was calculated by approximating the carbon content of the ferrite matrix at 0.012 wt %. The results obtained are summarized as follows: (1) the slopes of the first stage of

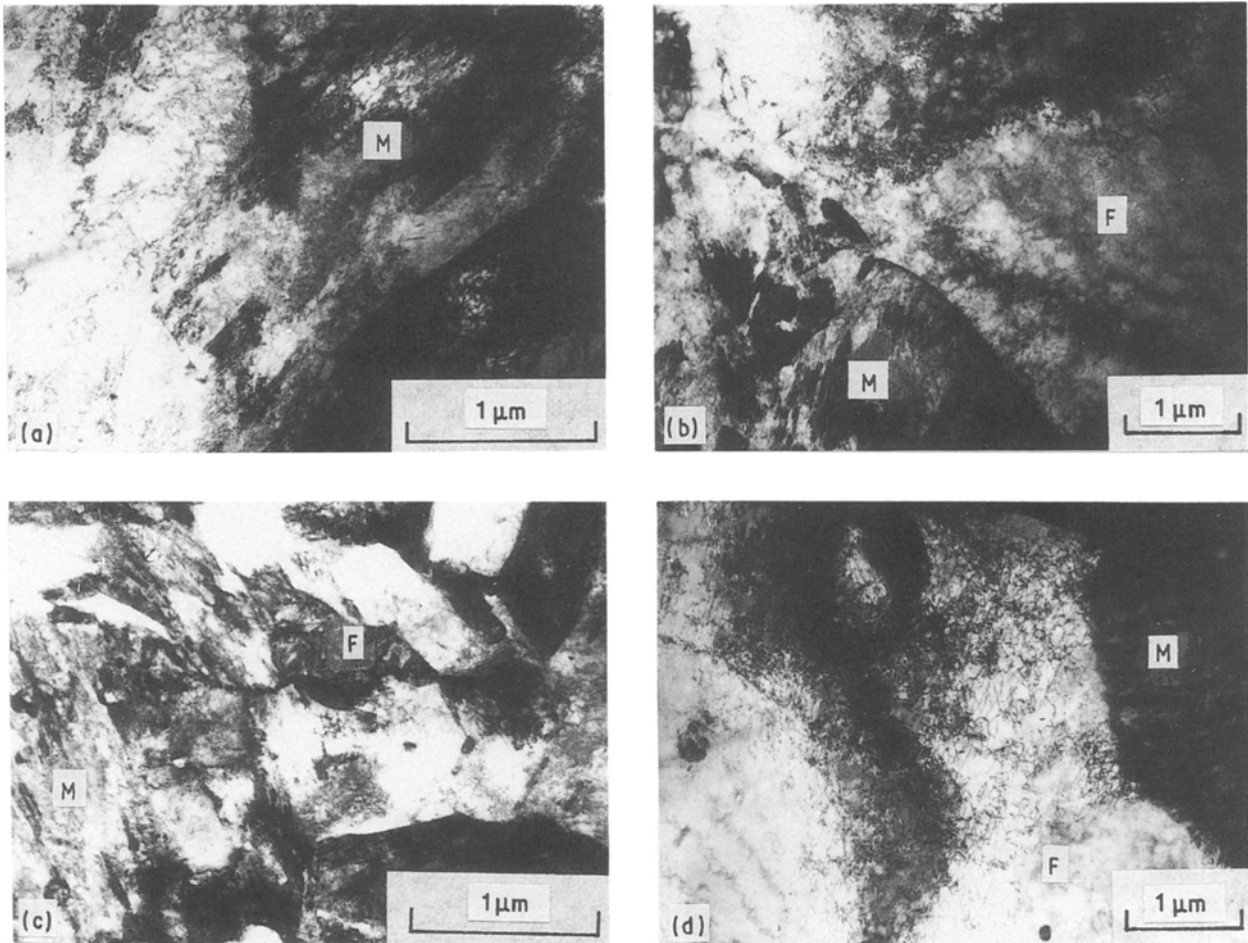


Figure 4 Microstructure of dual phase steels (TEM). (a) steel processed by heat treatment C; (b) steel processed by heat treatment A; (c) steel processed by heat treatment B; (d) steel processed by heat treatment C. M and F indicate martensite and ferrite regions, respectively.

TABLE II Mechanical properties of dual phase steels studied

Designation of heat treatment	V_m^* (%)	Strength		Yield ratio §	Elongation		Reduction in area (%)
		Y.S †	U.T.S. ‡ (MPa)		Uniform (%)	Total	
A1 ($T = 1023$ K)	9.3	345.0	511.1	0.68	16.3	53.7	42.0
A2 ($T = 1053$ K)	22.8	413.4	636.5	0.65	14.1	42.5	36.5
A3 ($T = 1073$ K)	28.3	426.5	667.6	0.64	13.2	41.5	35.8
B	22.7	413.2	654.8	0.63	16.0	52.9	45.1
C	23.0	324.7	568.3	0.57	16.2	51.9	42.1

* V_m volume fraction of martensite.

† YS 0.2% offset yield stress.

‡ UTS Ultimate tensile stress.

§ Yield ratio = YS/UTS.

the dual steel processed by heat treatments B and C are in good agreement with the slope of the single phase of ferrite and those of the second stage are approximately given by the law of a mixture of the individual slope of martensite and ferrite (Fig. 6). However, (2) the slopes of the first and second stages of the dual phase steel processed by heat treatment A are larger than that of FA steel and that given by the law of mixture of the individual slopes of ferrite and martensite, respectively (Fig. 5). This effect was prominent with an increased volume fraction of ferrite. From these results, it was found that in steels processed by heat treatments B and C, the first stage can be associated with the deformation of the ferrite matrix and the second stage is associated with the uniform strain of ferrite and martensite. The large slope observed in the first and second stages of the steel processed by heat treatment A is attributed to the fact that ferrite grains are plastically restrained by the surrounding martensite during plastic deformation. From the above results and arguments, the increased

0.2% offset yield stress of the steel processed by heat treatment A results from the fact that the initial flow stress is larger than the steels processed by heat treatments B and C as the result of plastic straining of ferrite by the surrounding martensite.

3.4. Fractography

Recent correlation investigation of the microstructures and mechanical properties of high strength steels having a mixed structure produced by phase transformation have shown that ductility is strongly affected by the fracture behaviour of the second phase [13-16]. Thus, in order to elucidate the effect of morphology of martensite on ductility, fractography was focused on the steels processed by heat treatments A and C, which exhibited a different morphology of the martensite at a similar volume fraction level of martensite. Fig. 7 shows examples of microcracks found behind the main fracture surface of the tensile specimen of two steels. For steel processed by heat treatment A microcracks being initiated at the interface between ferrite

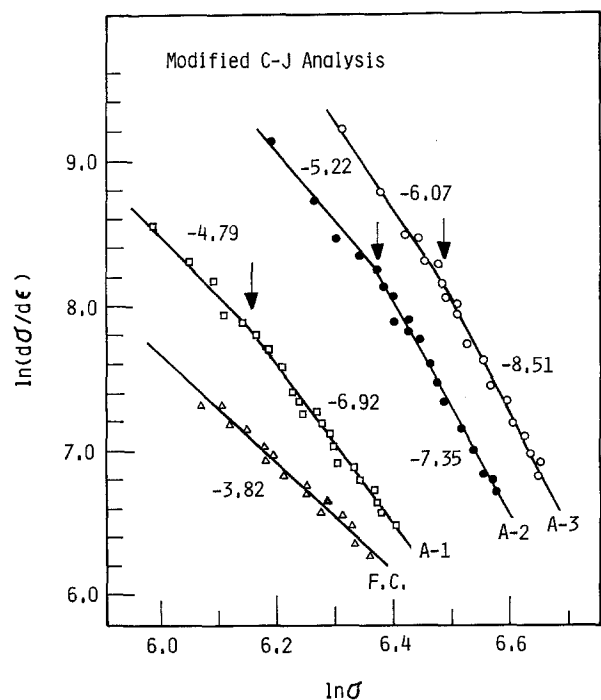


Figure 5 $\ln(d\sigma/d\epsilon)$ against $\ln \sigma$ curves for dual phase steels treated by heat treatment A and fully annealed Fe-0.1C steel (FA). Arrows indicate a knee. Numerals associated with curve represent the slope of the first stage and those of the second stage after the knee.

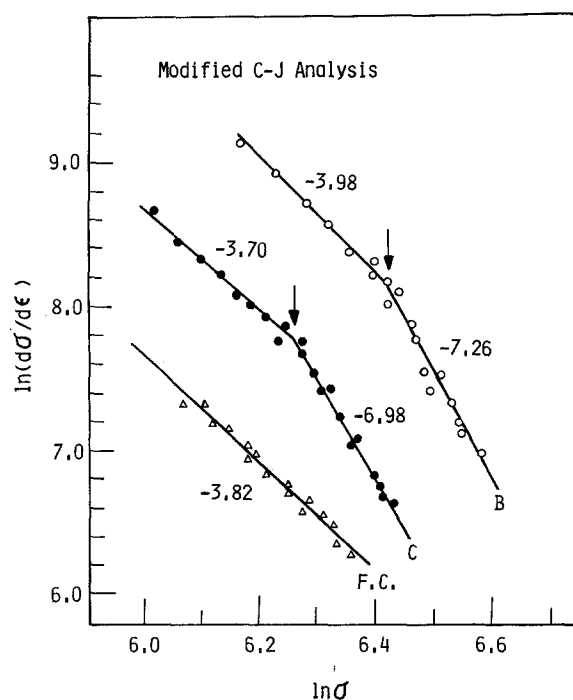


Figure 6 $\ln(d\sigma/d\epsilon)$ against $\ln \sigma$ curves for dual phase steels treated by heat treatments B and C and FA steel. Arrows indicate a knee. The numerals associated with the curve represent the slope of the first stage and those of the second stage after the knee.

TABLE III Comparison between measured and calculated slopes of first and second stages

Designation of heat treatment (V_m %)	Measured slope		Measured slope of ferrite* S_f^*	Measured slope of martensite S_T	Slope calculated from law of mixture ‡ $S_{mix} ‡$
	First stage	Second stage			
A2 (22.8)	- 5.22	- 7.35	- 3.82	- 20.10	- 7.53
B (22.7)	- 3.98	- 7.26	- 3.82	- 20.10	- 7.52
C	- 3.70	- 6.98	- 3.82	- 20.10	- 7.56

*Slope of fully annealed (F.A.) Fe-0.1 C steel.

†Slope of fully martensitic Fe-0.3 C steel.

‡ $S_{mix} = S_m V_m + S_f(100 - V_m)$.

and martensite were seen to propagate in a brittle manner through the ferrite grain (shown with arrows in Fig. 7a). For steels processed by heat treatment C, microcracks being initiated at martensite were also found (shown in arrows in Fig. 7b). This was reflected in the fracture surface shown in Fig. 8. That is, the fracture surface of steels processed by heat treatment A consisted of dimple fractures and brittle facets which seemed to be formed by brittle fracture in the ferrite region (Fig. 8a), but that of the steels processed by heat treatment C, all showed a well defined dimple pattern (Fig. 8b). From the fractography results, it was found that the difference of ductility between two steels is produced by whether microcracks are initiated at the ferrite or martensite sites. From stress-strain analysis, this will be determined by whether or not ferrite grains are plastically restrained by martensite. Thus, the detrimental effect on ductility of the steel processed by heat treatment A could be due to the fact that ferrite grains surrounded by martensite fractures in a brittle manner prior to martensite fracturing during necking. This is caused by the high local internal stress which is produced in the vicinity of the interface of the martensite and ferrite matrix as a result of plastic restraint of ferrite grains by the surrounding martensite during plastic deformation.

4. Conclusions

A study has been made of the effects of morphology (shape, size and distribution) on the second phase martensite on tensile properties of a dual phase Fe-0.1 C steel. The following conclusions can be drawn.

(1) Retention at the intercritical temperature of 1023 to 1073 K followed by ice-brine quenching (intercritical quenching treatments), whereby martensite appears to surround the ferrite grain, increased strength, but produced an increased yield ratio and decreased ductility.

(2) Incorporation of 1223 K direct ice-brine quenching prior to the intercritical quenching treatment at 1053 K gave rise to the distribution of fine spheroidized martensite in a refined ferrite matrix. The heat treatment significantly improved strength and ductility, but produced a somewhat increased yield ratio.

(3) Austenitization at a temperature of 1223 K followed by step quenching to 1023 K prior to ice-brine quenching, whereby martensite was randomly scattered in massive form in the ferrite matrix, gave the better combination strength and ductility and produced a decreased yield ratio.

(4) The above effect of the morphology of martensite on the tensile properties is discussed in terms of stress-strain analysis and fractography.

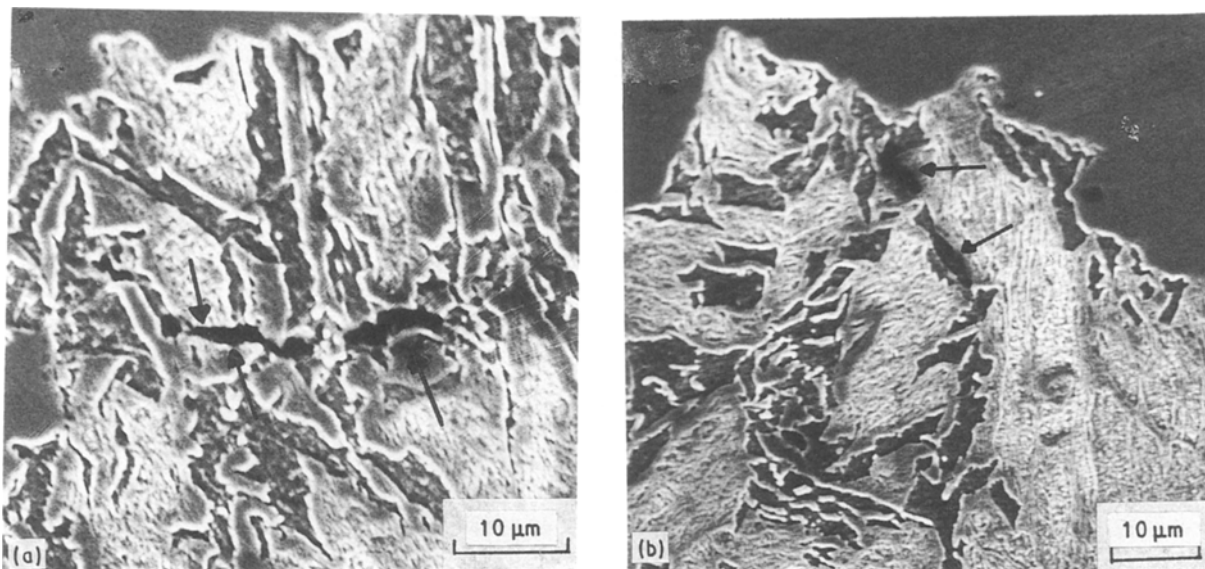


Figure 7 Examples of microcracks initiated behind the fracture surface (SEM). (a) steel processed by heat treatment A; (b) steel processed by heat treatment C. Arrows indicate microcracks.

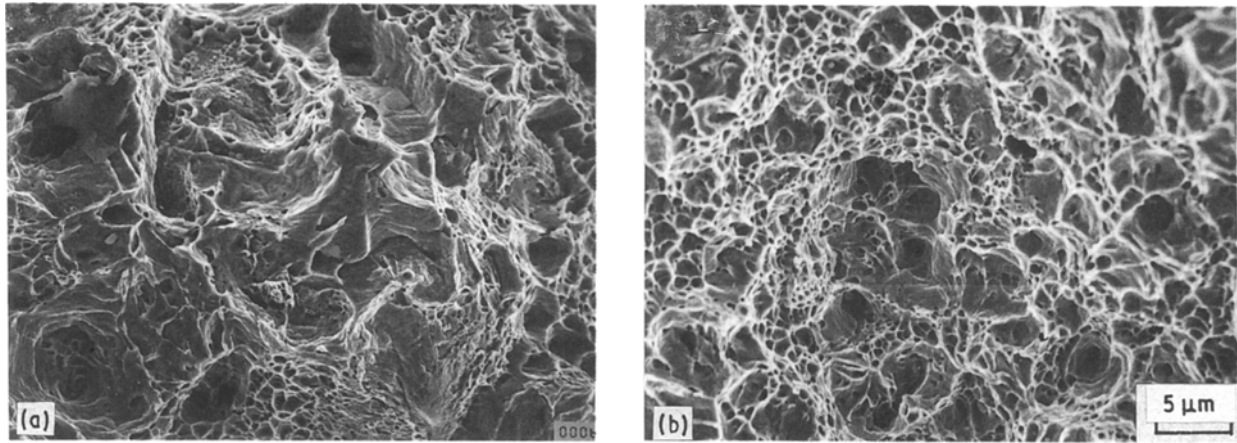


Figure 8 Fracture surface of dual phase steels (SEM). (a) steel processed by heat treatment A; (b) steel processed by heat treatment C.

References

1. T. MATSUOKA and K. YAMAMORI, *Met. Trans.* **6** (1975) 1613.
2. S. HAYAMI and T. FURUKAWA, "Micro-alloying 75" (Union Carbide Corporation, New York, 1977) p. 78.
3. R. G. DAVIES, *Met. Trans.* **9A** (1978) 41.
4. *Idem, ibid.* **9A** (1978) 451.
5. *Idem, ibid.* **9A** (1978) 671.
6. *Idem, ibid.* **10A** (1979) 113.
7. R. A. KOT and J. W. MORRIS (eds), "Structure and Properties of Dual Phase Steel" (AIME, New York, 1979).
8. A. T. DAVENPORT (eds), "Formable HSLA and Dual Phase Steels" (AIME, New York, 1979).
9. N. J. KIM and G. THOMAS, *Met. Trans.* **12A** (1981) 483.
10. J. DURNIN and K. A. RAIDA, *J. Iron Steel Inst.* **208** (1968) 60.
11. K. OKABAYASHI, Y. TOMITA and I. KUROKI, *J. Iron and Steel Inst. Jpn* **62** (1976) 662.
12. R. E. REED-HILL, W. R. CRIBB and S. N. MONTEIRO, *Met. Trans.* **4** (1973) 2665.
13. Y. TOMITA and K. OKABAYASHI, *Met. Trans.* **16A** (1985) 73.
14. *Idem, ibid.* **14A** (1983) 485.
15. *Idem, ibid.* **14A** (1983) 2387.
16. *Idem, ibid.* **16A** (1985) 83.

Received 7 July
and accepted 12 December 1989